Palladium(II) Complexes of the Thiosemicarbazone and *N*-Ethylthiosemicarbazone of 3-Hydroxypyridine-2-carbaldehyde: Synthesis, Properties, and X-Ray Crystal Structure

by **Mavroudis A. Demertzis***, **Paras Nath Yadav**, and **Dimitra Kovala-Demertzi***

Inorganic and Analytical Chemistry, Department of Chemistry, University of Ioannina, GR-45110 Ioannina
(phone: +30-32651-98425; fax: +30-32651-98792; e-mail: dkovala@cc.uoi.gr and mdemert@cc.uoi.gr)

Two novel, stable Pd^{II} complexes, compounds **3** and **4**, of two 3-hydroxypyridine-2-carbaldehyde thiosemicarbazones, **1** and **2**, resp., were prepared from Li_2PdCl_4. The single-crystal X-ray structure of complex **3** (=[Pd(**2**)Cl]) shows that the ligand monoanion coordinates in a planar conformation to the metal *via* the pyridyl N-, the imine N-, and the thiolato S-atoms. Intermolecular H-bonds, π–π, and CH$\cdots\pi$ interactions lead to a two-dimensional supramolecular assembly. The electronic, IR, UV/VIS, and NMR spectroscopic data of the two complexes are reported, together with their electrochemical properties. A sophisticated experimental procedure was used to determine the multiple dissociation constants of the ligands **1** and **2** by UV/VIS titration.

Introduction. – 3-Hydroxypyridine-2-carbaldehyde thiosemicarbazone (**1**) is a ribonucleotide reductase inhibitor affecting the enzyme's metal binding site. Compound **1** is a member of the so-called 'α-(*N*)-heterocyclic carbaldehyde thiosemicarbazones' (HCTs) [1], which are the most-potent known inhibitors of ribonucleoside diphosphate reductase. The reductive conversion of ribonucleotides to their deoxyribonucleotide counterparts is a particularly critical step in the synthesis of DNA, since deoxyribonucleotides are present in extremely low concentrations in mammalian cells. *Corey* and *Chiba* [2] have argued that an inhibitor of ribonucleotide reductase could be more effective than an inhibitor of DNA polymerase in blocking DNA synthesis. Thus, it seems reasonable that a strong inhibitor of ribonucleotide reductase, which is essential for cellular replication, would be a useful addition to the existing therapeutic anticancer agents.

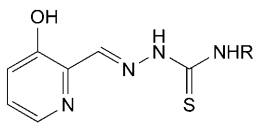

1 R = H
2 R = Et

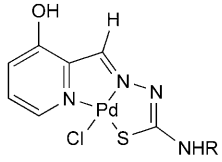

3 R = H
4 R = Et

Many HCTs have been reported to also exert tumor-inhibiting effects [3]. Early studies on structure–activity relationships of heterocyclic thiosemicarbazones have sug-

gested that antitumor activity directly correlates with their chelating ability [4]. Compounds **1** and 5-hydroxypyridine-2-carbaldehyde thiosemicarbazone have shown high activity in animal models, but were found to be readily glucuronidated and rapidly excreted [5]. The combination of **1** with Pt^{II} or Pd^{II} agents damaging DNA gives rise to synergistic inhibition of tumor growth by slowing down degradation processes through shielding of the coordinating metal by bulky ligands, and may lead to improvements in the effectiveness of cancer chemotherapy.

In earlier work, we investigated the Pd^{II} complexes formed with 2-acetylpyridine *N*-ethylthiosemicarbazone (HAc4Et) against Leukemia P388 cells. A high correlation between potency for SCE induction, effectiveness in cell-division delay ($P<0.01$) in normal human lymphocytes, both *in vitro* and *in vivo*, established antitumor activity in mice. These complexes were less cytotoxic and mostly more effective than the parent ligand, HAc4Et, acting synergistically [6]. The Pt^{II} complexes of HAc4Et were also found to exhibit cytotoxic potency in the very low micromolar range, being able to overcome the cisplatin resistance of A2780/Cp8 cells [7]. These complexes may be endowed with important anticancer properties since they elicit IC_{50} values in the same concentration range as the clinically used drug *cis*-DDP; moreover, they display cytotoxic activities in tumor lines resistant to *cis*-DDP.

In the present work, we have prepared and investigated the Pd^{II} complexes **3** and **4** of ligands **1** and **2**, respectively, to investigate whether these compounds act synergistically, the ultimate goal being to correlate chemical structure with biological activity [6–10]. This work is an extension of previously studied Pd^{II} and Pt^{II} complexes of thiosemicarbazones with potentially interesting biological activities [8–11].

Results and Discussion. – 1. *Ligand Dissociation Constants.* Both compound **1** and its Et congener **2**, designated here as H_2A, possess two protic functions, NH and OH, as well as a pyridine N-atom susceptible to single protonation. Therefore, in aqueous solution, three independent conjugate acid–base pairs may be present. The dissociation constants were determined by UV/VIS titration, as described elsewhere [12], the analysis being based on *Eqns. 1–3*. The resulting pK_a values and details of the calibration curves are collected in *Table 1*, and selected titration curves are shown in *Fig. 1*.

$$\varepsilon_o = A_{H_2A} + \frac{1}{K_{a1}}(A_{H_3A^+} - A_o)[H_3O^+] \quad (1)$$

$$\varepsilon_o = A_{H_2A} - K_{a2}\frac{A_o - A_{HA^-}}{[H_3O^+]} \quad (2)$$

$$\varepsilon_o = A_{A^{2-}} + \frac{1}{K_{a3}}(A_{HA^-} - A_o)[H_3O^+] \quad (3)$$

2. *Synthesis.* Compounds **1** and **2** were synthesized by means of the *Heinert–Martell* reaction (*Scheme*) [13]. The corresponding Pd^{II} complexes **3** and **4** were prepared by reacting lithium tetrachloropalladate (Li_2PdCl_4) – prepared *in situ* from $PdCl_2$ and LiCl – with the appropriate ligand in MeOH solution in a molar ratio of 1:1. For details, see the *Exper. Part*.

Table 1. *Analytical Parameters of the UV/VIS-Titration Graphs for the Determination of the Acid–Base Properties of Ligands* **1** *and* **2**

Ligand	RSD of slope [%]	Confidence limit of slope	n	R	λ_{obs} [nm]	pK_a[a])
1	1.56	$3.27\times10^{3}\pm1.21\ 10^{2}$	9	0.9991	376	3.51 ± 0.02
	−1.69	$-4.60\times10^{-8}\pm1.68\times10^{-9}$	15	0.9982	376	7.34 ± 0.02
	6.45	$1.13\times10^{12}\pm2.31\times10^{11}$	5	0.9938	384	12.05 ± 0.09
2	2.21	$4.37\times10^{3}\pm2.22\times10^{2}$	10	0.9980	376	3.64 ± 0.02
	−0.83	$-5.61\times10^{-8}\pm1.08\times10^{-9}$	10	0.9978	376	7.25 ± 0.01
	6.42	$8.42\times10^{11}\pm1.72\times10^{11}$	4	0.9945	385	11.91 ± 0.10

[a]) Three values per ligand are given (pK_a(1)–pK_a(3)) in the order of acidity.

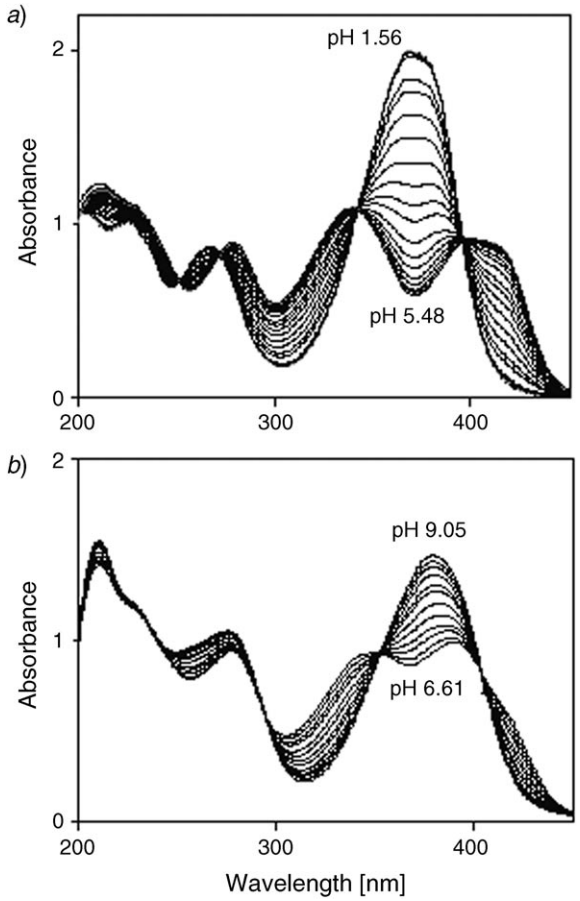

Fig. 1. *UV/VIS Titration curves of the ligand* **1** *at* a) *pH 1.56–5.48* (H_3A^+/H_2A pair) *and* b) *pH 6.61–9.05* (H_2A/HA^- pair). For details, see *Exper. Part*.

3. *Structural Characterization.* Complex **4** was recrystallized from MeCN to furnish orange prisms suitable for single-crystal X-ray analysis (*Figs. 2–4*). Selected inter-

Scheme

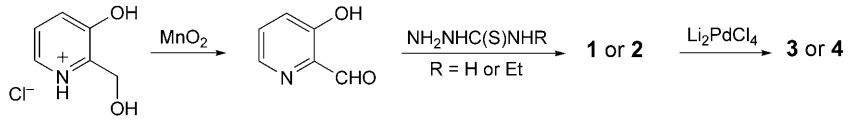

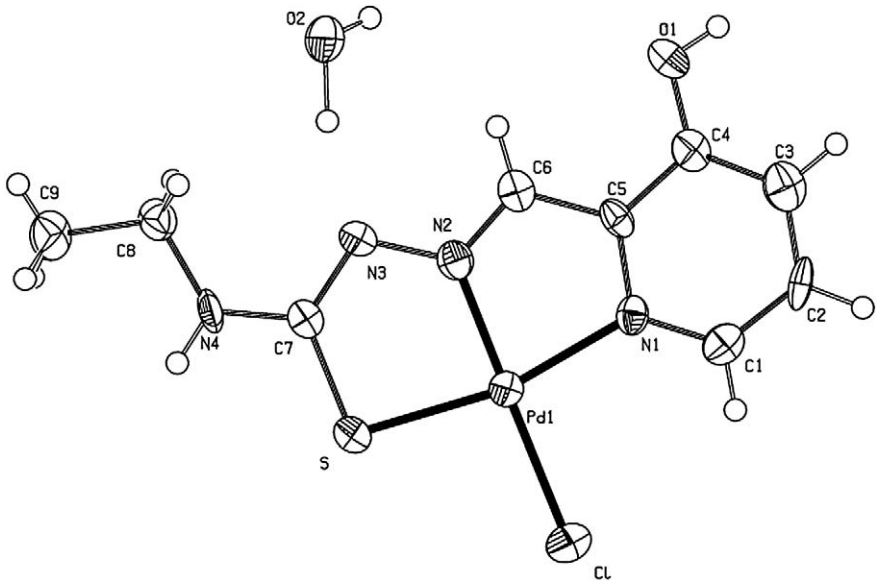

Fig. 2. *X-Ray crystal structure of the Pd^{II} complex* **4**

atomic distances and bond angles are collected in *Table 2*. Anionic **2** acts as a tridentate ligand coordinating to the Pd^{II} center through the pyridyl N-atom, N(1), the azomethine N-atom, N(2), and the thiolato S-atom. The ligand shows a (*Z*,*E*,*Z*)-configuration for these three donor centers, respectively. The S–C bond distance is consistent with an increased single-bond character, and both thioamide C=N distances indicate increased double-bond character. The ligand is basically planar, as indicated by the dihedral angle between the mean planes of the pyridyl ring and the chelate ring Pd–S–C–N–N, as well as between the mean planes of the pyridyl ring and Pd–N–C–C–N, with values of 3.5(3) and 2.3(4)°, respectively.

Within the crystal, complex **4** is arranged in a head-to-tail fashion with a neighboring complex to form dimeric substructures stabilized by strong double π–π interactions *via* Pd(1)–S–C(7)–N(3)–N(2) {Cg(1)} → Pd(1)–N(2)–C(6)–C(5)–N(1) {Cg(2)}, the rings Cg(1) and Cg(2) facing each other at a typical stacking distance of 3.601(5) Å (*Fig. 4*, *Table 3*). The dimers are also connected by CH–π interactions. Atom H–C(8) is directed towards the symmetry-related $(2-x, -y, 2-z)$ pyridyl ring, with a distance of 3.531(11) Å (*Table 3*). Thereby, one molecule of H_2O participates in H-bonding. Strong intermolecular H-bonding occurs between the O(2)-atom of H_2O and H–O(1) $(2-x, 1/2+y, 5/2-z)$ [O(1)···O(2), 2.645(11) Å; O(1)···H, 1.86 Å; O(2)···H–

Table 2. *Selected Interatomic Distances* (in Å) *and Angles* (in °) *for* **4**. The following symmetry transformations were used to generate equivalent atoms: #1: $(-x+1, y+1/2, -z+3/2)$; #2: $(-x+1, y-1/2, -z+3/2)$.

Pd(1)–N(2)	1.933(8)	N(2)–Pd(1)–N(1)	81.3(3)
Pd(1)–N(1)	2.039(7)	N(2)–Pd(1)–S	85.0(3)
Pd(1)–S	2.236(3)	N(1)–Pd(1)–S	166.3(2)
Pd(1)–Cl	2.317(2)	N(2)–Pd(1)–Cl	179.2(3)
S–C(7)	1.739(8)	N(1)–Pd(1)–Cl	98.2(2)
N(3)–C(7)	1.339(11)	S–Pd(1)–Cl	95.51(9)
N(3)–N(2)	1.387(11)	C(7)–S–Pd(1)	95.5(3)
N(2)–C(6)	1.289(12)	C(7)–N(3)–N(2)	110.7(7)
N(1)–C(1)	1.330(11)	C(6)–N(2)–N(3)	119.0(7)
N(1)–C(5)	1.371(10)	C(6)–N(2)–Pd(1)	117.0(7)
O(1)–C(4)	1.315(10)	N(3)–N(2)–Pd(1)	123.9(6)
N(4)–C(7)	1.334(12)	C(1)–N(1)–C(5)	116.7(8)
N(4)–C(8)	1.473(11)	C(1)–N(1)–Pd(1)	132.1(6)
		C(5)–N(1)–Pd(1)	111.2(6)

Table 3. *π–π and CH–π Interactions for* **4**. Cg(1), Cg(2), and Cg(3) refer to the centroids Pd(1)–S–C(7)–N(3)–N(2), Pd(1)–N(2)–C(6)–C(5)–N(1), and N(1)–C(1)–C(2)–C(3)–C(4)–C(5), resp.

π–π Interactions (Cg(*I*) → Cg(*J*))	Distance between ring centroids [Å]	Angle β between ring centroids [°]	Cg(*I*)–Perp[a]) [Å]	Cg(*J*)–Perp[b]) [Å]
Cg(1) → Cg(1)[i c])	3.933(4)	24.98	3.565	3.565
Cg(1) → Cg(2)[i]	3.601(5)	10.59	3.551	3.540
Cg(2) → Cg(1)[i]	3.601(5)	10.59	3.540	3.551
CH–π Interactions	H···Cg [Å]	C–H···Cg [°]	C···Cg [Å]	
C(8)–H(8B) → Cg(3)[ii]	2.73	140.0	3.531 (11)	

[a]) Cg(*I*)–Perp is the perpendicular distance of Cg(*I*) on ring *J* and [b]) Cg(*J*)–Perp is the perpendicular distance of Cg(*J*) on ring *I*. [c]) Symmetry transformations: [i] = $(1-x, -y, 2-z)$; [ii] = $(2-x, -y, 2-z)$.

Table 4. *Intramolecular H-Bonds for* **4**. D and A refer to 'donor' and 'acceptor', resp.

D–H	A	D···A [Å]	H···A [Å]	D–H···A [°]
O(2)–H	N(3)	2.822(9)	1.71	163.0
N(4)–H	Cl[iii a])	3.464(8)	2.61	173.0
O(1)–H[iv a])	O(2)	2.645(11)	1.86	161.0
C(1)–H	S[v]	3.547(10)	2.76	143.0

[a]) Symmetry transformations: [iii] = $(1-x, -1/2+y, 3/2-z)$; [iv] = $(2-x, 1/2+y, 5/2-z)$; [v] = $(1-x, 1/2+y, 3/2-z)$.

O(1), 161°] and between N(3) and H–O(2) [N(3)···O(2), 2.822(9) Å; N(3)···H, 1.71 Å; O(2)–H–N(3), 163°] (*Table 4*). Also, there is an intermolecular H-bond between the H–N(4) and the coordinated Cl ligand, and another one between H–C(1) and

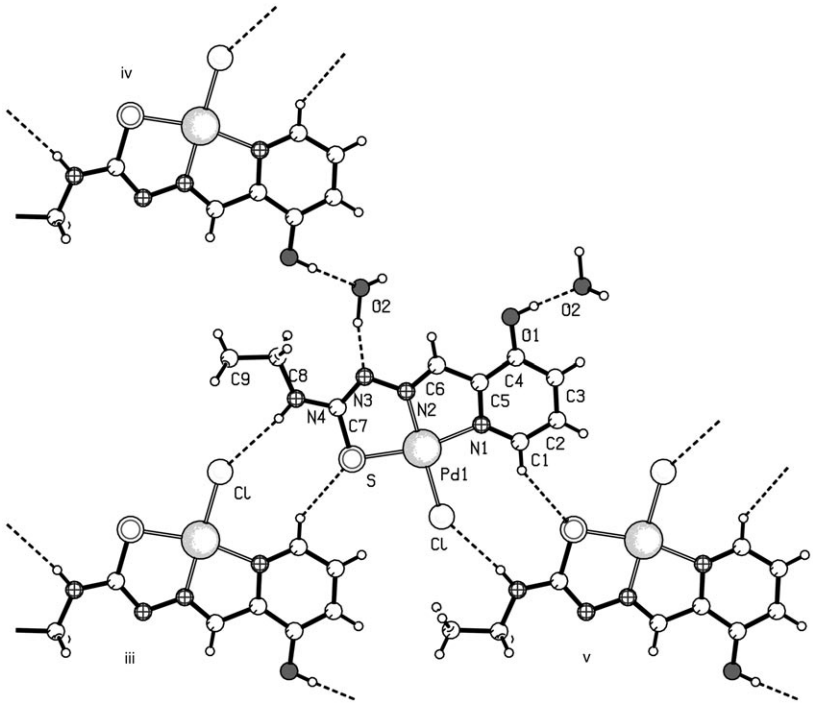

Fig. 3. *Intermolecular H-bonds in the crystal structure of* **4**. Symmetry operations: [iii] = (1 − *x*, −1/2 + *y*, 3/2 − *z*), [iv] = (2 − *x*, 1/2 + *y*, 5/2 − *z*), [v] = (1 − *x*, 1/2 + *y*, 3/2 − *z*).

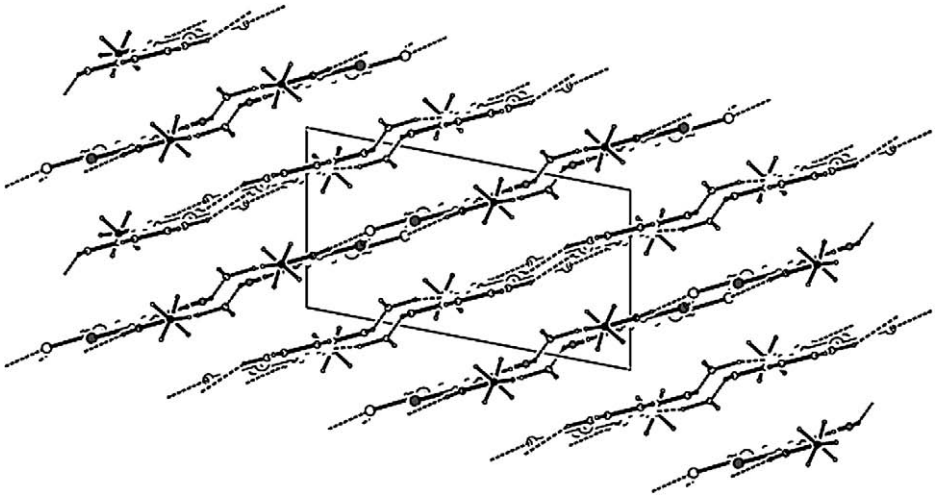

Fig. 4. *Crystal packing of* **4** *viewed along the* b*-axis of the unit cell*

the S-atom (*Fig. 3*, *Table 4*). These two intermolecular H-bonds connect the monomers, which results in an infinite two-dimensional network (*Fig. 4*). Thereby, each complex is partly hydrophilic at its outer surface, and partly hydrophobic at the interior. Strong intermolecular H-bonding, π–π, and CH–π interactions help to stabilize the structure.

4. *Spectroscopic Properties.* 4.1. *IR Spectra*. The coordination of the azomethine N-atom to the Pd^{II} center was suggested in the IR spectra of complexes **3** and **4**, relative to those of the free ligands, by a shift of the ν(C=N) band to lower frequencies, along with the occurrence of a ν(N–N) band to higher frequency. Furthermore, the presence of a band at *ca.* 450–500 cm^{-1} was assigned to ν(Pd–N). The thioamide band, which contains considerable ν(CS) character, was less intense in the complexes and found at a lower frequency, suggesting coordination of the metal through sulfur after deprotonation. Coordination of the thiolato S-atom was further indicated by a decrease in the energy of the thioamide band, as well as by the presence of a band at *ca.* 400 cm^{-1} assignable to ν(Pd–S). As expected, greater energy decreases in the thioamide band occurred for the anionic form of the ligand owing to the C–S entity formally becoming a single bond. The 'breathing motion' of the pyridine ring was shifted to higher frequency upon complexation, which is consistent with coordination of the pyridine N-atom. An IR band at 1229 or 1221 cm^{-1} for **1** and **2**, respectively, was assigned to ν(C–O). This band was found to be shifted to 1185 and 1197 cm^{-1}, respectively, in the spectra of the corresponding complexes **3** and **4**, which indicates that coordination of the carbonyl O-atom does not occur. The relatively low energy of the ν(C–O) vibration in the spectra of **1**–**4** indicated that the carbonyl O-atom is involved in H-bonding [14].

4.2. *NMR Spectra*. Peak assignments were based on 2D-NMR data (^{1}H,^{1}H-COSY, ^{1}H,^{13}C-HMQC, ^{1}H,^{13}C-HMBC). In the ^{1}H-NMR spectra of the ligands **1** and **2**, H–N(3) resonated at *ca.* δ(H) 11.50, indicating that this H-atom is involved in H-bonding [15][16]. This resonance was absent in the spectra of the corresponding complexes, which indicated deprotonation of H–N(3) and, thus, anionic semicarbazone moieties.

In the ^{1}H-NMR spectra of the Pd^{II} complexes **3** and **4**, both H–C(1) and the formyl H-atom H–C(6) were shifted upon coordination, which indicated variations in the electron density at positions 1 and 6. These two signals were shifted upfield, in accord with an increased electron density at these sites in the complexes. However, due to π-back-bonding from Pd^{II} to the imine function, an upfield shift of these resonances was observed. These data indicate that the complexes are formed by ligand deprotonation followed by metallation, a structural motive that seems to be stable both in the solid state and in DMSO solution. The C=S resonances of the thiosemicarbazone moieties in the free ligands resonated at δ(C) 177.1–178.4. In the complexes, downfield shifts were observed, indicating decreased electron density from the thiolato C-atoms [15][16].

4.3. *UV/VIS Spectra*. The electronic spectra of complexes **3** and **4** were indicative of square-planar geometries. In the visible region, three spin-allowed S $\rightarrow$ S (d $\rightarrow$ d) transitions can be expected [8]. However, strong charge-transfer (CT) transitions prevented the observation of all these predicted bands. The very intense band at *ca.* 25,000–26,000 cm^{-1} in the spectra of the Pd^{II} complexes was assigned to the HOMO $\rightarrow$ LUMO transition. The HOMO is a mixed orbital centered on Pd and the two donor atoms, d(Pd)/p(S)/p(Cl). In contrast, the LUMO is mainly centered on the pyridyl ring. The observed

strong bands at 27,000–29,000 cm^{-1} were assigned to intraligand (IL) and CT transitions.

The UV spectrum of complex **3** was also computed by single-point calculations (ZINDO/1 singly excited interaction configuration) [14][17] based on the X-ray structural data of the complex.

5. *Electrochemical Studies.* The cyclic voltammogram (CV) of the ligands **1** and **2** in DMF solution exhibited an irreversible negative cathodic wave at -1.272 and -1.306 V, respectively. This results from the reduction of the imine and thioamide groups present in the thiosemicarbazone moiety, and these values are comparable to those observed for other thiosemicarbazones [14]. The CVs of the complexes **3** and **4** showed irreversible reductions at -1.344 and -1.360 V, respectively. The reduction potentials of **3** and **4** was more negative than that of the corresponding ligands, and a decrease in the order **1** < **2** < **3** < **4** indicated that the reduction process in the complexes is more difficult than in the free ligands.

The electrochemical data suggest that the reduction of **1**–**4** might be regarded as more or less taking place on the pyridyl ring. The electron transfer from Pt is directed to the LUMO π^* orbital, which is a mixed orbital centered mainly on the pyridine. The oxidation waves for **1** and **2** were observed at $+0.657$ and $+0.618$ V, respectively, and those for **3** and **4** at $+0.339$ and $+0.295$ V, respectively. Oxidation is also associated with a ligand-based process, and oxidized products are formed. The oxidation potentials of **1**–**4** increase in the order **1** > **2** > **3** > **4**. Thus, reduction of ligands **1** and **2** is more easily accomplished than in either **3** or **4**, while the oxidation processes is more difficult. However, in the range from $+1.5$ to -2.5 V, additional peaks were observed.

Experimental Part

General. – Solvents were purified and dried according to standard procedures. UV/VIS Spectra (including near-IR): *JASCO V-570* spectrophotometer; λ_{max} in cm^{-1} (ε in l mol^{-1} cm^{-1}). FT-IR (including far-IR) Spectra: *Nicolet 55XC* spectrophotometer, KBr pellets (4000–400 cm^{-1}) and nujol mulls dispersed between polyethylene disks (400–40 cm^{-1}). ^{1}H- and ^{13}C-NMR Spectra: *Bruker AMX-400* spectrometer, at 250.13 and 62.90 MHz, resp., at ambient temp. in (D_6)DMSO; δ in ppm rel. to residual solvent signals (δ(H) 2.49 and 7.24, resp.). Elemental analyses (C,H,N,S) were performed on a *Carlo-Erba EA-1108* apparatus at the University of Ioannina. Analyses of Pd and Cl were performed in our laboratory by gravimetric and potentiometric techniques, resp.

Electrochemical Measurements. All measurements were made with an *AUTOLAB PGSTAT30* potentiostat using a Pt microsphere as working electrode, a Pt-wire auxiliary electrode, and an Ag/AgCl reference electrode in a three-electrode configuration. Ferrocene was added at the end of each experiment and used as an internal standard. All potentials are reported rel. to the Ag/AgCl reference electrode and ferrocinium/ferrocene (Fe^+/Fc; $E_{1/2} = 0.173$ V) in DMF at a scan rate 100 mV s^{-1}. $Et_4N^+ClO_4^-$ (0.1M) was used as supporting electrolyte, with 10^{-3} M solns. of the complexes. All experiments were carried out under N_2 atmosphere.

3-Hydroxypyridine-2-carbaldehyde Thiosemicarbazone (**1**). Commercially available 3-hydroxy-(2-hydroxymethyl)pyridine hydrochloride was oxidized with MnO_2, prepared by heating $MnCO_3$ for 12 h at 300°, according to [13] to afford 3-hydroxypyridine-2-carbaldehyde in 62% yield as a yellow powder (m.p. 77°). The aldehyde (2 mmol) was then reacted with a soln. of thiosemicarbazide (2 mmol) in EtOH (6 ml) at 60° for 16 h. Then, the mixture was kept in a refrigerator overnight. The resulting precipitate was filtered off, washed with cold EtOH, and dried *in vacuo* over silica gel at 40–50° for 4 h to afford the title compound. Yield 75%. Bright-yellow powder. M.p. 209°. UV/VIS (DMF): 28,820 (44,100). IR: 3555*s*, 3451*m* (ν(OH)); 3291*m*, 3194*m* (ν(NH_2, NH)); 1639*s* (ν(C=N)); 1229*s* (ν(C–O));

1098*s* (ν(NN)); 827*s* (ν(C=S)). ^{1}H-NMR[1]): 11.56 (*s*, H–N(3)); 8.14 (*d*, H–C(1)); 7.24 (*m*, H–C(2), H–C(3); 9.67 (*s*, OH); 8.35 (*s*, H–C(6)); 8.04/8.25 (br. *s*, NH_2). ^{13}C-NMR[1]): 178.4 (C(7)); 153.8 (C(4)); 144.1 (C(6)); 141.3 (C(1)); 137.9 (C(5)); 125.6 (C(2)); 124.5 (C(3)). Anal. calc. for $C_7H_8N_4OS$ (196.04): C 42.8, H 4.1, N 28.6, S 16.3; found: C 42.6, H 3.9, N 28.2, S 16.0.

3-Hydroxypyridine-2-carbaldehyde N-*Ethylthiosemicarbazone* (**2**). A soln. of 3-hydroxypyridine-2-carbaldehyde (2 mmol) in EtOH (7 ml) was treated with a soln. of *N*-ethylyhiosemicarbazide (2 mmol) in dist. H_2O (3 ml). The mixture was heated at reflux for 2 h, and then left standing in a refrigerator overnight. The resulting precipitate was filtered off, washed with cold EtOH, and dried *in vacuo* over silica gel at 50° for 4 h. Yield: 80%. Bright-yellow powder. M.p. 201°. UV/VIS (DMF): 28,700 (43,600). IR: 3298*m* (ν(OH)); 32254*m*, 3119*m* (ν(NH_2, NH)); 1597*s* (ν(C=N)); 1221*s* (ν(C–O)); 1085*s* (ν(NN)); 836*m* (ν(C=S)). ^{1}H-NMR[1]): 11.53/14.19 (*s*, H–N(3)); 9.82 (br. *s*, OH); 8.48 (*t*, J=7.5, H–N(4)); 8.37 (*s*, H–C(6)); 8.12 (*d*, H–C(1)); 7.24 (*m*, H–C(3), H–C(2)); 3.56 (*q*, J=6.9, CH_2); 1.12 (*t*, J=7.1, Me). ^{13}C-NMR[1]): 177.3/177.1 (C(7)); 153.66/153.30 (C(4)); 141.3/139.1 (C(1)); 138.16/139.6 (C(5)); 128.15 (C(3)); 125.40/143.4 (C(6)); 124.5/126.3 (C(2)); 38.8 (Me); 14.6/14.5 (CH_2). Anal. calc. for $C_9H_{12}N_4OS$: C 48.2, H 5.4, N 24.9, S 14.3; found: C 48.2, H 5.3, N 24.7, S 14.4.

Chloro(3-hydroxy-2-pyridinecarboxaldehyde Thiosemicarbazonato)palladium(II) ([Pd(**1**)Cl]; **3**). To lithium tetrachloropalladate (1.2 mmol), prepared *in situ* from $PdCl_2$ and LiCl, in MeOH (9 ml) was added a soln. of ligand **1** (1 mmol) in MeOH (8 ml). The mixture was stirred for 24 h at r.t., and then left standing in a refrigerator for 24 h. The resulting orange precipitate was filtered off, washed with cold MeOH and Et_2O, and dried *in vacuo* over silica gel, and then at 70° *in vacuo* over P_4O_{10} for 2 h. Yield: 79%. Orange powder. M.p. 317° (dec.). UV/VIS (DMF): 28,605 (sh, 39,600), 26,970 (40,900), 25,720 (41,500). IR: 3514*w*, 3403*m* (ν(OH)); 3310 (br.), 3156 (br.) (ν(NH_2, NH)); 1626*s* (ν(C=N)); 1185*s* (ν(C–O)); 1045*w* (ν(NN)); 708*w* (ν(C=S)); 499*s* (ν(PdN)); 416*m* (ν(PdS)); 351*s* (ν(PdCl)); 302*m* (ν(PdN_{py})). ^{1}H-NMR[1]): 11.52 (*s*, OH); 8.02 (*d*, J=7.6, H–C(1)); 7.82 (br. *s*, NH_2); 7.71 (*s*, H–C(6)); 7.50 (br., H–C(3), H–C(2)). ^{13}C-NMR[1]): 181.97 (C(7)); 153.88 (C(4)); 145.57 (C(6)); 142.75 (C(1)); 139.87 (C(5)); 127.30 (C(2), C(3)). Anal. calc. for $C_7H_7ClN_4OPdS$: C 24.9, H 2.1, Cl 10.5, N 16.6, Pd 31.6, S 9.5; found: C 25.0, H 2.1, Cl 10.5, N 16.5, Pd 31.5, S 9.6.

Chloro(3-hydroxypyridine-2-carboxaldehyde N-*Ethylthiosemicarbazonato)palladium(II) Monohydrate* ([Pd(**2**)Cl]·H_2O; **4**). Prepared as described above for **3**, but using ligand **2**. Yield 85%. Orange powder. M.p. 230° (dec.). UV/VIS (DMF): 28,075 (sh, 40,000), 26,740 (sh, 41300), 25,125 (42,200). IR: 3417 (br, ν(OH)); 3335*w*, 3281*s* (ν(NH_2, NH)); 1606*s* (ν(C=N)); 1197*s* (ν(C–O)); 1060*w* (ν(NN)); 757*m* (ν(C=S)); 506*m* (ν(PdN)); 408*m* (ν(PdS)); 335*m* (ν(PdCl)); 296*m* (ν(PdN_{py})). ^{1}H-NMR[1]): 8.11 (*s*, H–N(4)); 7.98 (*d*, H–C(1)); 7.77 (*s*, H–C(6)); 7.44, 7.55 (*m*, H–C(3), H–C(2)); 4.84 (br. *s*, OH); 3.23 (*q*, J=7.8, CH_2); 1.07 (*t*, J=7.1, Me). ^{13}C-NMR[1]): 178.29 (C(7)); 154.04 (C(4)); 145.51 (C(6)); 143.79 (C(1)); 139.80 (C(5)); 127.76 (C(3)); 127.30 (C(2)); 41.57 (Me); 14.55 (CH_2). Anal. calc. for $C_9H_{11}ClN_4OPdS·H_2O$: C 28.2, H 3.4, Cl 9.3, N 14.6, Pd 27.8, S 8.4; found: C 28.3, H 3.5, Cl 9.3, N 14.7, Pd 27.3, S 8.4.

X-Ray Crystallography[2]). Slow evaporation of a MeCN solution of **4** provided an orange prismatic crystal, which was mounted on a glass fiber and used for data collection. X-ray diffraction data were collected on a *Bruker SMART APEX* diffractometer with graphite-monochromated MoK_α radiation (λ=0.71073 Å). Cell constants and an orientation matrix for data collection were obtained by least-squares refinement of the diffraction data from 25 reflections in the range $2.12° < \omega < 25.00°$. Data were collected at 293 K, and corrected for *Lorentz* and polarization effects. A semi-empirical absorption correction (ω-scans) was made. The structure was solved by direct methods (SHELXS97) [18], and refined by the full-matrix least-squares method on all F^2 data using the WinGX version of the SHELXL97 software [19]. All H-atoms were located in their calculated positions (C–H bond length

---

[1]) Trivial atom numbering (see *Fig. 2*).

[2]) The crystallographic data of **4** ($C_9H_{11}ClN_4OPdS$) have been deposited with the *Cambridge Crystallographic Data Centre* as supplementary publication No. CCDC-293433. Copies of the data can be obtained, free of charge, at http://www.ccdc.cam.ac.uk/data_request/cif.

Table 5. *Crystallographic Data for* **4**

Empirical formula	$C_9H_{11}ClN_4OPdS$
M_r [g/mol]	365.13
Crystal system	Monoclinic
Space group	$P2_1/c$
Unit-cell dimensions:	
a, b, c [Å]	7.2280(10), 13.925(2), 13.246(2)
a, β, γ [°]	90, 100.920(10), 90
V [Å^3]	1309.1(3)
Z	4
D_{calc} [g/cm^3]	1.853
μ(MoK_α) [1/mm]	1.780
F(000)	720
Crystal Size [mm]	$0.20\times0.20\times0.30$ mm
Temperature [K]	293(2) K
λ [Å]	0.71073
θ Range for data collection	2.14–25.00°
Limiting indices	$0<h<8, -1<k<14, -14<l<14$
Reflections collected, unique	2634, 2238 ($R_{int}=0.0602$)
Absorption correction	none
Refinement method	Full-matrix least-squares on F^2
Data, restraints, parameters	2238, 0, 174
GoF on F^2	1.004
Final R [$I>2\sigma(I)$]	$R1=0.0554$, $wR2=0.1046$
R (all data)	$R1=0.1151$, $wR2=0.1247$
Largest diff. peak and hole	0.693, −0.821 e/A^3

0.93–0.97 Å), and refined using a riding model, except for Ow-H1 and Ow-H2, which were located through *Fourier*-difference synthesis. Molecular graphics were performed with PLATON 2001 [20]. A summary of the crystal data, experimental details, and refinement results are to be found in *Table 5*.

Determination of Dissociation Constants. Dist. H_2O, obtained from a borosilicate auto-still (*BIGASA Spa*, Model *BE-115/R*), was used throughout. Stock solns. of *ca.* 10^{-4} M (concentration not exactly known [21]) were prepared for each ligand by suspending the appropriate amount of each compound in warm H_2O for some hours, until sufficient dissolution was achieved. Then, the solns. were cooled to r.t., insoluble material being removed by filtration, and finally diluted to the required concentration. From each stock soln., four working solns. (A–D) of exactly the same, but unknown, ligand concentration (*ca.* 5×10^{-5} M) were prepared. Soln. A contained 0.01M KOH and 0.09M KCl, soln. B contained 0.1M HCl and 0.1M KCl, soln. C contained 0.1M HCl, and soln. D contained 0.1M KOH and 0.1M KCl. During a typical UV/VIS titration of A with B, C, and D, many samples of nearly 5×10^{-5} M ligand concentration, having different pH values, but constant ionic strengths ($\mu=0.1$, see below), were gradually prepared. Their pH values were measured, and the related absorption spectra were recorded by transferring a portion of each sample into a UV/VIS cuvette. Specifically, A was titrated within a jacketed vessel against B until neutralization (pH 7.00). Other amounts of A were again added into the vessel whenever necessary to correct and obtain a desired pH value. Samples with pH < 7.00 were made by adding C in the titrated soln. of the vessel. Amounts of D were added into the vessel whenever corrections for pH < 7.00 were necessary. It must be emphasized that it was no problem to partly or totally transfer the content of the cuvette into a vessel, or pouring it elsewhere. Further, soln. A can have different concentrations of KOH and KCl, provided the sum of them is equal to 0.1M. Soln. B contained various HCl concentrations;

C, in addition to HCl, may also contain KCl, the sum of their concentrations being 0.1M; finally, *D* can only have different concentrations of KOH. All UV/VIS absorption spectra and pH measurements were made at 25° on a *JASCO 590 UV-VIS-NIR* spectrophotometer and a *Methrom-691* pH meter, resp.

Example: Find the ionic strength of a sample after addition of V_B ml of *B*, which is *a* M in HCl and 0.1M in KCl, to V_A ml of *A*, containing *b* M and *c* M of KOH and KCl, with $b+c=0.1$, resp. Soln. *B* contains $a\times V_B$ mmol of HCl that react with $a\times V_B$ mmol of KOH of *A* and gives $a\times V_B$ mmol of KCl. After addition of *B* to *A*, the soln. contains $(b\times V_A)-(a\times V_B)$ mmol of KOH, but no HCl. The total concentration c_{tot} of KOH plus KCl in soln. is $c_{tot}=(bV_A-aV_B+aV_B+cV_A+0.1\ V_B)/(V_A+V_B)=0.1$. The ionic strength of the soln. (sample) is also 0.1, equal to c_{tot}, since mono-monovalent electrolytes are used. At the equivalence point, the soln. contains only 0.1M of KCl, and below pH 7.00, it contains a total concentration of HCl + KCl equal to 0.1M. Therefore, the ionic strength of the solution during the titration process is constant and equal to that of the analyte soln. (*A*).

We thank the NMR center of the University of Ioannina and Dr. *V. Exarchou*. Dr. *R. Vargas* is kindly acknowledged for recording the X-Ray data at the X-ray crystallography center of the University of Babes-Bolyai University, Cluj-Napoca, Romania.

REFERENCES

[1] J. G. Cory, A. H. Cory, G. Rappa, A. Lorico, M. C. Liu, T.-S. Lin, A. C. Sartorelli, *Biochem. Pharmacol.* **1994**, *48*, 335.
[2] J. G. Cory, P. Chiba, in 'Inhibitor of Ribonucleoside Diphosphate Reductase Activity', Eds. J. G. Cory, A. M. Cory, Pergamon Press, Oxford, 1989, pp. 245–264.
[3] F. A. French, J. E. Blanz, *J. Med. Chem.* **1974**, *17*, 172, and refs. cit. therein.
[4] A. E. Liberta, D. X. West, *Biometals* **1992**, *5*, 121; A. G. Quiroga, J. M. Pérez, I. López-Solera, J. R. Masaquer, A. Luque, P. Román, A. Edwards, C. Alonso, C. Navarro-Ranninger, *J. Med. Chem.* **1998**, *41*, 1399.
[5] D. R. Richardson, *Crit. Rev. Oncol./Hemat.* **2002**, *42*, 267, and refs. cit. therein.
[6] A. Papageorgiou, Z. Iakovidou, D. Mourelatos, E. Mioglou, L. Boutis, A. Kotsis, D. Kovala-Demertzi, A. Domopoulou, D. X. West, M. A. Demertzis, *Anticancer Res.* **1997**, *17*, 247; D. Kovala-Demertzi, A. Domopoulou, M. A. Demertzis, G. Valle, A. Papageorgiou, *J. Inorg. Biochem.* **1997**, *68*, 147.
[7] D. Kovala-Demertzi, P. Nath Yadav, M. A. Demertzis, M. Coluccia, *J. Inorg. Biochem.* **2000**, *78*, 347.
[8] Z. Iakovidou, E. Mioglou, D. Mourelatos, A. Kotsis, M. A. Demertzis, A. Papageorgiou, P. Nath Yadav, D. Kovala-Demertzi, *Anticancer Drugs* **2001**, *12*, 65.
[9] D. Kovala-Demertzi, M. A. Demertzis, V. Varagi, A. Papageorgiou, D. Mourelatos, E. Mioglou, Z. Iakovidou, A. Kotsis, *Chemotherapy* **1998**, *44*, 421.
[10] D. Kovala-Demertzi, M. A. Demertzis, J. R. Miller, C. Papadopoulou, C. Dodorou, G. Filousis, *J. Inorg. Biochem.* **2001**, *86*, 555.
[11] D. Kovala-Demertzi, M. A. Demertzis , E. Filiou, A. A. Pantazaki, P. N. Yadav, Y. Zheng, D. A. Kyriakidis, *Biometals* **2003**, *16*, 411
[12] P. N. Yadav, M. A. Demertzis, D. Kovala-Demertzi, A. Castineiras, D. X. West, *Inorg. Chim. Acta* **2002**, *332*, 204.
[13] D. Heinert, A. E. Martell, *J. Am. Chem. Soc.* **1959**, *81*, 3933.
[14] P. Nath Yadav, M. A. Demertzis, D. Kovala-Demertzi, S. Skoulika, D. X. West, *Inorg. Chim. Acta* **2003**, *349*, 30.
[15] M. A. Demertzis, S. K. Hadjikakou, D. Kovala-Demertzi, A. Koutsodimou, M. Kubicki, *Helv. Chim. Acta* **2000**, *83*, 2787.
[16] V. Dokorou, D. Kovala-Demertzi, J. P. Jasinski, A. Galani, M. A. Demertzis, *Helv. Chim. Acta* **2004**, *87*, 1940.
[17] HYPERCHEM, Release 6.01 for Windows, Molecular Modeling System, *Hypercube, Inc*., Gainsville, FL, 2000.
[18] G. M. Sheldrick, *Acta Crystallogr., Sect. A* **1990**, *46*, 467; G. M. Sheldrick, SHELXL97 and SHELXS97, University of Göttingen, Germany.

[19] L. J. Farrugia, *J. Appl. Cryst.* **1999**, *32*, 837.
[20] A. L. Spek, PLATON: Program for the Automated Generation of a Variety of Geometrical Entities, University of Utrecht, The Netherlands, 2001.
[21] D. Kovala-Demertzi, M. Demertzis, P. Nath Yadav, A. Castineiras, D. X. West, *Transition Met. Chem.* **1999**, *24*, 642.

Received April 7, 2006